

## Impurity-Induced Infrared Absorption in a Monatomic fcc Lattice\*

T. P. MARTIN†

*Institute of Optics and Department of Physics and Astronomy, University of Rochester, Rochester, New York*

(Received 16 February 1967)

The infrared absorption by a low concentration of defects in a monatomic fcc lattice has been calculated. The host crystal was assumed to be composed of uncharged atoms interacting only with their nearest neighbors by means of central harmonic forces. The substitutional-defect atom differed from the host atoms in its mass, nearest-neighbor force constant, and effective charge. Calculations were made using effective-charge parameters based on a rigid, charged defect and uncharged host atoms and on an uncharged, deformable defect and deformable host atoms. Both the localized-mode frequencies and the band-mode absorption coefficient were expressed in terms of the Green's functions of Lifshitz. The real and imaginary parts of the 12 necessary Green's functions of the perfect crystal were calculated assuming rigid atoms. The vectorlike localized-mode frequencies were calculated for defects with various masses and force constants. The coefficient of absorption by band modes was calculated as a function of frequency for defects with various masses, force constants, and effective charges. The model gives fair agreement with exploratory absorption measurements on presumably applicable systems, i.e., Ar:Kr and Ar:Xe.

### STATEMENT OF PROBLEM

THERE are two important selection rules governing the one-phonon absorption of light by a perfect crystal. Only those normal modes with the frequency and wavelength of the incident light can be excited. This means that of the  $3N$  modes of vibration, only a long-wavelength mode of each transverse-optical branch will absorb. A monatomic fcc crystal has no optical branches and none of the modes in the acoustical branches will satisfy these selection rules. Any departure of the lattice from translational symmetry, though, will result in the breakdown of the selection rule requiring the phonon and photon to have the same wavelength, and both localized modes and acoustical-band modes of the appropriate point symmetry will contribute to the absorption. We have calculated such absorption for the following model using Green's-function techniques. The host crystal is composed of uncharged atoms arranged in a fcc lattice. These atoms interact with one another by means of nearest-neighbor, central harmonic forces. Charged and uncharged defects are included substitutionally. These defects have a different mass than the host atoms. The force constant describing the interaction of the defect with its nearest neighbors is also different. The concentration of impurities is assumed to be low. Although a rigid-atom approximation is used to determine the dynamics of the imperfect crystal, the effective charge of the normal modes is estimated using a shell model of the atoms as well as using a charged, rigid-defect model.

### LOCALIZED MODES

In the harmonic approximation, the absorption coefficient due to a localized mode is an isolated  $\delta$  function of frequency. The formalism for determining these

eigenfrequencies has been developed by Lifshitz<sup>1</sup> and is outlined below in order to establish notation.

The Green's-function technique gives an exact solution to large, local changes of an otherwise solvable problem. Suppose we know the solutions of the dynamical equations of an unperturbed lattice. In the harmonic approximation, for a monatomic lattice, these equations can be written

$$\frac{1}{M} \sum_{l',\beta} \Phi_{\alpha\beta}{}^{ll'} X_{\beta l'}{}^a = \omega_a^2 X_{\alpha l}{}^a, \quad (1)$$

where  $M$  is the atomic mass and  $\omega_a$  the frequency of mode  $a$ . The matrix  $\mathbf{X}$  defines the transformation from atomic displacement coordinates to normal coordinates. Specifically,  $X_{\alpha l}{}^a$  relates the displacement of the  $l$ th atom in the  $\alpha$  direction to the amplitude of normal mode  $a$ . We wish to find the motion of an imperfect lattice whose dynamical equations can be written

$$\frac{1}{M} \left[ \sum_{l',\beta} \Phi_{\alpha\beta}{}^{ll'} Y_{\beta l'}{}^b + \sum_{l',\beta} \Delta_{\alpha\beta}{}^{ll'} Y_{\beta l'}{}^b \right] = \omega_b^2 Y_{\alpha l}{}^b. \quad (2)$$

Using our knowledge of the solutions of the unperturbed crystal, Eq. (1), it is possible to obtain a more convenient dynamical equation for the imperfect lattice,

$$\mathbf{Y}^b = \mathbf{G}(\omega_b^2) \Delta \mathbf{Y}^b, \quad (3)$$

where

$$G_{\alpha\alpha'}(l,l'; \omega^2) = \left[ (M\omega^2 \mathbf{I} - \Phi)^{-1} \right]_{\alpha\alpha'}{}^{ll'} = \sum_a \frac{X_{l\alpha}{}^a X_{l'\alpha'}{}^{a*}}{\omega^2 - \omega_a^2}. \quad (4)$$

Equation (4) defines the Green's function of any harmonic lattice. We will be particularly interested in the Green's function of a perfect lattice, i.e., a lattice with translational symmetry. For a perfect lattice it is well known that<sup>2</sup>

$$X_{l\alpha}{}^{jk} = (MN)^{-1/2} \mathbf{E}_\alpha(\mathbf{k}, j) e^{i\mathbf{k} \cdot \mathbf{r}_l^0}, \quad (5)$$

\* Research supported in part by the National Science Foundation. Based in part on a thesis submitted to the University of Rochester in partial fulfillment of requirements for the Ph.D. degree.

† Present address: Department of Physics, University of Illinois, Urbana, Illinois.

<sup>1</sup> I. M. Lifshitz, *Nuovo Cimento Suppl.* **3**, 716 (1956).

<sup>2</sup> A. A. Maradudin, E. W. Montroll, and G. H. Weiss, *Solid State Phys. Suppl.* **3**, 30 (1963).

where the eigenstates  $a$  are now conveniently labeled by a wave vector  $\mathbf{k}$  and a branch  $j$ .  $E_\alpha(\mathbf{k}, j)$  is the  $\alpha$  component of the polarization vector for mode  $\mathbf{k}, j$ .  $\mathbf{U}_l^0$  is the equilibrium position vector of the  $l$ th atom. Substitution into Eq. (4) gives the Green's function of a perfect crystal,

$$G_{\alpha\beta}(L_x, L_y, L_z; \omega^2) = (MN)^{-1} \times \sum_{j\mathbf{k}} \frac{E_\alpha(\mathbf{k}, j)E_\beta(\mathbf{k}, j)}{\omega^2 - \omega_j^2(\mathbf{k})} e^{i\mathbf{k} \cdot \mathbf{U}(L_x, L_y, L_z)}. \quad (6)$$

Here we have used the notation

$$\mathbf{U}(L_x, L_y, L_z) = \mathbf{U}_l^0 - \mathbf{U}_{l'}^0. \quad (7)$$

Equation (3) may be considered an eigenvalue problem with eigenvalues equal to 1. If the Green's function is assumed a function of  $\omega$ , that  $\omega$  which satisfies Eq. (3) will be  $\omega_b$ , the eigenvalue of Eq. (2). The additional work

of finding the Green's functions is more than offset by a convenient reduction in the number of dimensions of the new eigenvalue problem. The secular determinant implied by Eq. (3) has the dimensions (in our model  $39 \times 39$ ) of the nonzero submatrix of  $\Delta$  which we will call  $\delta$ . If  $\mathbf{g}$  represents the corresponding submatrix of  $\mathbf{G}$ , then the secular equation can be written<sup>3</sup>

$$|\mathbf{1} - \mathbf{g}\delta| = 0. \quad (8)$$

A further reduction in the number of dimensions is obtained by a transformation  $\mathbf{R}$  to the symmetry coordinates of the defect and its nearest neighbors. Under such a transformation, Eq. (8) factors in exactly the same way as the secular equation of a molecule. Since we are interested in only the optically active localized modes, we shall solve only the  $4 \times 4$  vectorlike factor, Eq. (9) below. This factor is obtained by a transformation to the symmetry coordinates shown in Fig. 1.

$$|\mathbf{1} - \mathbf{g}\delta| = 0 = \begin{vmatrix} -Ag_{xx}(000) + 8Bg_{xx}(110) & +8BDg_{xx}(000) & 0 & -8BDg_{xx}(000) \\ +8Bg_{xy}(110) + 1 & -8BDg_{xx}(110) & & +8BDg_{xy}(110) \\ & -8BDg_{xy}(110) & & +8BDg_{xx}(110) \\ -8ADg_{xx}(110) & +8Bg_{xx}(110) - BJ + 1 & 0 & -8Bg_{xx}(110) + BL \\ +8BDJ + 8BDL & -BL & & +BJ \\ -2Ag_{xx}(011) + 8BF & +16BDg_{xx}(011) - 8BDF & 1 & -16BDg_{xx}(011) \\ +8Bg_{xy}(211) & -8BDg_{xy}(211) & & +8BDg_{xy}(211) \\ & & & +8BDF \\ +8ADg_{xy}(110) & -8Bg_{xy}(110) + BL - BK & 0 & +8Bg_{xy}(110) \\ -8BDL + 8BDK & & & +BK + 1 - BL \end{vmatrix}. \quad (9)$$

Here we have used the following notation. The mass and nearest-neighbor force constant of a host atom are  $M$  and  $\gamma$ , respectively, of the defect atom,  $M'$  and  $\gamma'$ . Moreover,

$$D = 1/\sqrt{8}, \quad \Delta M = M - M', \quad \Delta\gamma = \gamma - \gamma', \quad (10)$$

$$A = \Delta M \omega^2 - 4\Delta\gamma, \quad B = -\Delta\gamma/2,$$

and

$$\begin{aligned} J &= g_{xx}(000) + g_{xx}(200) + g_{xx}(020) + g_{xx}(220) \\ &\quad + 2g_{xx}(011) + 2g_{xx}(211), \\ L &= 2g_{xy}(211) + g_{xy}(220), \\ K &= -g_{xx}(000) - g_{xx}(220) + g_{xx}(200) + g_{xx}(020) \\ &\quad + 2g_{xy}(110) - 2g_{xy}(112), \\ F &= g_{xx}(110) + g_{xx}(121). \end{aligned} \quad (11)$$

Using Green's functions calculated by Kagle and Maradudin,<sup>4</sup> the  $4 \times 4$  determinant in Eq. (9) was evaluated as a function of frequency for various defect parameters. For each set of parameters the value of the

determinant was found either never to pass through zero or to pass through zero only once. These roots, which correspond to localized-mode frequencies, are plotted above the abscissa in Fig. 2. The maximum frequency of a perfect-lattice mode has been denoted by  $\omega_L$ , which in our model is equal to  $(8\gamma/M)^{1/2}$ . The localized-mode frequencies for the mass defect (necessarily vectorlike) have been calculated by Maradudin.<sup>5</sup> These frequencies agree with the  $\Delta\gamma/\gamma = 0$  curve in Fig. 2.

Once we have obtained the localized-mode frequencies, Eq. (3) allows us to determine the relative motion of the atoms within the defect space. Table I shows the amount of each of the symmetry coordinates in the eigenvector for several choices of defect parameters. Of course, the atoms outside the defect space will also participate in the localized mode. Since the motion of these atoms has been left undetermined, a normalization condition cannot be set up to establish the absolute magnitudes of the displacements. The projected eigenvectors defined in Table I have been arbitrarily normalized to 1. An examination of Table I reveals a few

<sup>3</sup> A. A. Maradudin, *Solid State Phys.* **18**, 278 (1966).

<sup>4</sup> B. S. Kagle and A. A. Maradudin, Westinghouse Research Laboratories, Research Memo 64-929-442-M1, 1964 (unpublished).

<sup>5</sup> A. A. Maradudin, in *Phonons and Phonon Interactions*, edited by T. A. Bak (W. A. Benjamin, Inc., New York, 1964).

TABLE I. Eigenvectors  $\{S_i\}$  of vectorlike localized modes.

$\Delta\gamma/\gamma^a$	$\Delta M/M^b$	$\frac{\omega_{loc}^c}{L}$	$S_1$	$S_2$	$S_3$	$S_4$
0.8	0.90	1.026	0.994	-0.068	0.023	0.082
0.8	0.95	1.427	0.999	-0.022	0.002	0.027
0.4	0.70	1.068	0.961	-0.177	0.049	0.206
0.4	0.85	1.448	0.995	-0.066	0.007	0.073
-0.4	-0.10	1.015	0.616	-0.485	0.174	0.596
-0.4	0.20	1.090	0.809	-0.380	0.096	0.439
-0.4	0.50	1.285	0.949	-0.227	0.034	0.217
-0.4	0.60	1.408	0.970	-0.174	0.020	0.169
-0.8	-0.60	1.024	0.491	-0.542	0.184	0.657
-0.8	0.50	1.446	0.953	-0.210	0.023	0.218

<sup>a</sup>  $\gamma$  is the nearest-neighbor force constant of a host atom.

<sup>b</sup>  $M$  is the mass of a host atom.

<sup>c</sup>  $\omega_L$  is the maximum frequency of a perfect-lattice mode and  $\omega_{loc}$  is the localized-mode frequency.

generalizations regarding the character of the localized modes. As the localized-mode frequency increases, the eigenvector becomes more localized, i.e., the motion of the impurity atom  $S_1$  predominates. At lower frequencies, approximately equal amounts of  $S_2$  and  $S_4$  also contribute to the eigenvector. The symmetry coordinate  $S_3$  does not seem to play an important role in defining the motion of the localized modes.

## BAND-MODE ABSORPTION

### Mathematical Formulation

A calculation of the infrared absorption due to the band modes in an imperfect lattice is considerably more difficult than determining the localized-mode frequencies. Many of the  $3N$  band modes can absorb infrared radiation (about  $9N/16$  of the modes are optically active<sup>6</sup>). It would be possible to solve this problem using many-body theory in the form of thermal double-time

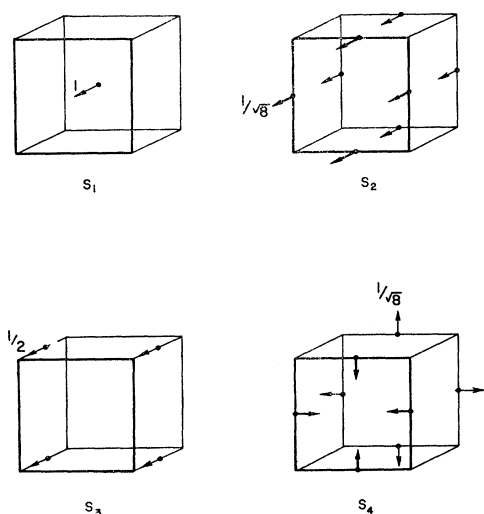
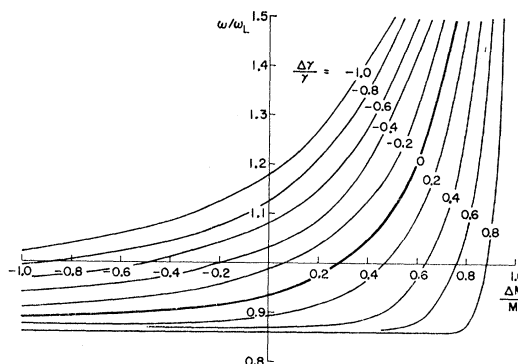


FIG. 1. Vectorlike symmetry coordinates.

<sup>6</sup> R. S. Knox, *Solid State Commun.* **4**, 453 (1966).

FIG. 2. Resonance  $D$  and vectorlike localized-mode frequencies.

Green's functions and Kubo's theory of linear response. In fact, such techniques have been used in solving the mass-defect problem.<sup>7,8</sup> However, we approach our problem through the semiclassical theory of radiation which, because of its long use, gives considerable physical insight.

The interaction Hamiltonian used in the semiclassical treatment of this problem may be written in a simplified form if we assume that the wavelength of the radiation is large compared to the electronic displacements from a lattice site  $U_l^0$  and to the nuclear displacements,

$$H' = \sum_{l,j} \left[ \frac{ie\hbar}{m c} \nabla_{U_j} \cdot \mathbf{f} - \frac{iz_l \hbar}{M_l c} \nabla_{U_l} \cdot \mathbf{f} \right] A_0 e^{i\mathbf{k} \cdot \mathbf{U}_l^0 - i\omega t}, \quad (12)$$

where  $\mathbf{r}_{l,j}$  is the position of the  $j$ th electron on the  $l$ th atom,  $\mathbf{U}_l$  is the position of the  $l$ th nucleus,  $m$  is the mass of the electron,  $M_l$  is the mass of the  $l$ th nucleus,  $z_l$  is the charge on the  $l$ th nucleus, and

$$\mathbf{A} = A_0(\omega) \mathbf{f} e^{i(\mathbf{k} \cdot \mathbf{U}_l^0 - \omega t)} \quad (13)$$

is the vector potential of the electromagnetic field. Using this interaction Hamiltonian, time-dependent perturbation theory leads to an absorption coefficient given by<sup>9</sup>

$$K_p(\omega) = \frac{D 4\pi^2}{3n\hbar c} \left( \frac{n^2 + 2}{3} \right)^2 \omega_p |\mathfrak{M}_p|^2 g(\omega_p, \omega), \quad (14)$$

where  $D$  is the density of defects,  $n$  is the index of refraction of the host,  $c$  is the speed of light,  $g(\omega_p, \omega)$  is the shape function, and

$$\mathfrak{M}_p = \int \phi_0^* \left[ \sum_{jl} -e\mathbf{r}_{jl} + z_l \mathbf{U}_l \right] e^{i\mathbf{k} \cdot \mathbf{U}_l^0} \phi_p d\mathbf{r} d\mathbf{U}. \quad (15)$$

Here,  $\phi_0$  is the wave function of the ground state of the

<sup>7</sup> A. A. Maradudin, in *Astrophysics and the Many Body Problem* (W. A. Benjamin, Inc., New York, 1963).

<sup>8</sup> W. M. Hartmann, Ph.D. thesis, Oxford University, 1966 (unpublished); W. M. Hartmann and R. J. Elliott (to be published).

<sup>9</sup> M. Lax and E. B. Burstein, *Phys. Rev.* **97**, 39 (1955).

crystal and  $\phi_p$  the wave function of an excited state. Using the Born-Oppenheimer wave functions for the stationary states of the crystal, the dipole matrix element, Eq. (15), becomes for a purely vibrational transition

$$\mathfrak{M}_p = \Theta_0^*(\mathbf{U})\mathbf{M}(\mathbf{U})\Theta_p(\mathbf{U})d\mathbf{U}, \quad (16)$$

where

$$\mathbf{M}(\mathbf{U}) = \left[ \sum_l z_l \mathbf{U}_l - \int \theta_a^*(\mathbf{r}, \mathbf{U}) \times \sum_{j,l} \epsilon \mathbf{r}_{jl} \theta_a(\mathbf{r}, \mathbf{U}) \right] e^{i\mathbf{k} \cdot \mathbf{U}_l^0} d\mathbf{r} \quad (17a)$$

and

$$\phi_p(\mathbf{r}, \mathbf{U}) = \Theta_p(\mathbf{U})\theta_0(\mathbf{r}, \mathbf{U}). \quad (17b)$$

We have previously assumed that the electronic wave function varies smoothly and slowly with the nuclear displacements  $\mathbf{u}_l$ :

$$\mathbf{u}_l = \mathbf{U}_l - \mathbf{U}_l^0. \quad (18)$$

Expanding  $\theta_a(\mathbf{r}, \mathbf{U})$  in powers of  $\mathbf{u}_l$ , we have the result

$$M_\alpha = \sum_{l,\beta} e_l^{\alpha\beta} \mathbf{u}_{l\beta} e^{i\mathbf{k} \cdot \mathbf{U}_l^0}, \quad (19)$$

where the effective charge is

$$e_l^{\alpha\beta} = z_l - e \sum_{l',j} \int \theta_a^{l\beta}(\mathbf{r}) r_{l'\alpha j} \theta_a^0(\mathbf{r}) d\mathbf{r}. \quad (20)$$

Physically,  $e_l^{\alpha\beta}$  is the  $\alpha$  component of the dipole moment of the crystal induced by a unit displacement of the  $l$ th atom in the  $\beta$  direction. It is shown below that in our model only the defect atom and its nearest neighbors will have a nonzero effective charge. Since the incident radiation has a wavelength on the order of  $10^5$  lattice sites, we can write Eq. (19) as

$$M_\alpha = \sum_{l\beta} e_l^{\alpha\beta} \mathbf{u}_{l\beta}. \quad (21)$$

The total absorption can now be obtained by summing Eq. (14) over all modes of the perturbed crystal,

$$K(\omega) = \frac{D4\pi^2}{n\hbar c} \left( \frac{n^2+2}{3} \right)^2 \sum_p \omega_p |\mathfrak{M}_p|^2 g(\omega_p, \omega), \quad (22)$$

where

$$(\mathfrak{M}_p)_x = \int \Theta_0(\mathbf{u}) \sum_{l\beta} e_l^{x\beta} \mathbf{u}_{l\beta} \Theta_p(\mathbf{u}) d\mathbf{u}. \quad (23)$$

If we expand  $\mathbf{u}$  in normal modes  $\mathbf{Q}$  of the imperfect crystal,

$$\mathbf{u} = \mathbf{Y}\mathbf{Q}, \quad (24)$$

the integral in Eq. (23) is easily evaluated, giving

$$(\mathfrak{M}_p)_x = \left( \frac{\hbar}{2\omega_p} \right)^{1/2} \sum_{l,\beta} e_l^{x\beta} Y_p^{l\beta}. \quad (25)$$

Making a transformation  $\mathbf{R}$  to symmetry coordinates in the space of the defect, this becomes

$$(\mathfrak{M}_p)_x = \left( \frac{\hbar}{2\omega_p} \right)^{1/2} \sum_m e_m^x \sum_{l\beta} (R^{-1})_m^{l\beta} Y_p^{l\beta}, \quad (26)$$

where

$$e_m^x = \sum_{l,\beta} e_l^{x\beta} R_m^{l\beta} \quad (27)$$

is an effective charge parameter of the  $m$ th symmetry coordinate. Substituting Eq. (26) into Eq. (22), we obtain

$$K(\omega) = \frac{2\pi^2 D}{nc} \left( \frac{n^2+2}{3} \right)^2 \sum_{m,m'} e_m^x e_{m'}^x \sum_{l,l',\beta,\beta'} (R^{-1})_m^{l\beta} \times \left\{ \sum_p Y_p^{l\beta} Y_p^{*l'\beta'} g(\omega_p, \omega) \right\} R_{l,\beta}^{m'} R_{l',\beta'}^{m'}. \quad (28)$$

It is mathematically convenient to represent the line shape of a single vibrational mode by a  $\delta$  function. This is consistent with our harmonic model. A further justification is that there are many normal frequencies very close together, and we will be interested in the contribution of all modes in a finite frequency interval to the absorption coefficient. Using the well-known representation of the  $\delta$  function,

$$g(\omega_p, \omega) = \delta(\omega_p, \omega) = \frac{2\omega}{\pi} \lim_{\epsilon \rightarrow 0} \text{Im}(\omega^2 - \omega_p^2 - i\epsilon)^{-1}, \quad (29)$$

we can write the expression in curly brackets in Eq. (28) as

$$\left\{ \sum_p Y_p^{l\beta} Y_p^{*l'\beta'} g(\omega_p, \omega) \right\} = \lim_{\epsilon \rightarrow 0} \text{Im} \frac{2\omega}{\pi} \sum_p \frac{Y_p^{l\beta} Y_p^{*l'\beta'}}{\omega^2 - \omega_p^2 - i\epsilon}. \quad (30)$$

This expression contains a complex in-band Green's function for an imperfect crystal,

$$\mathfrak{G}_{\beta\beta'}(l, l'; \omega_i - i\epsilon) = \sum_p \frac{Y_p^{l\beta} Y_p^{*l'\beta'}}{\omega^2 - \omega_p^2 - i\epsilon}. \quad (31)$$

The submatrix  $\mathfrak{G}_0$  corresponding to the space of the defect can be written in terms of the submatrices of matrices of  $\mathbf{A}$  and  $\mathbf{G}$ :

$$\mathfrak{G}_0 = (\mathbf{I} - \mathbf{g}\mathfrak{G})^{-1} \mathbf{g}. \quad (32)$$

Using Eqs. (30), (31), and (32) in Eq. (28), we obtain

$$K(\omega) = \frac{4\pi D\omega}{nc} \left( \frac{n^2+2}{3} \right)^2 \sum_{m,m'} e_m^x e_{m'}^x \times \lim_{\epsilon \rightarrow 0} \text{Im} \{ [\mathbf{R}^{-1}(\mathbf{I} - \mathbf{g}\mathfrak{G})\mathbf{R}]^{-1} \mathbf{R}^{-1} \mathbf{g} \mathbf{R} \}_{m,m'}. \quad (33)$$

The Green's-function matrix of an imperfect crystal is factored in the defect space by a transformation  $\mathbf{R}$ , like the secular equation of the corresponding "defect molecule." Since only the effective-charge parameters

of those symmetry coordinates that transform like a vector are nonzero,<sup>10</sup> the sum in Eq. (33) is over only these symmetry coordinates.

The integrated absorption coefficient including band-mode and localized-mode absorption can be obtained from Eq. (28). If the shape function  $g(\omega_p, \omega)$  is replaced by a  $\delta$  function  $\delta(\omega_p - \omega)$  and if  $K(\omega)$  is integrated over all frequencies including any localized modes, we obtain in atomic-displacement coordinates

$$\int K(\omega) d\omega = \frac{D2\pi^2}{nc} \left( \frac{n^2+2}{3} \right)^2 \sum_{l, \alpha} e_l^{\alpha x} e_{l', \alpha' x} \times \sum_p Y_p^{l\alpha} Y_p^{*l'\alpha'} \quad (34)$$

Using the closure relation

$$\sum_p Y_p^{l\alpha} Y_p^{*l'\alpha'} = \frac{\delta_{l,l'} \delta_{\alpha,\alpha'}}{M_l}, \quad (35)$$

Eq. (34) simplifies to

$$\int K(\omega) d\omega = \frac{D2\pi^2}{nc} \left( \frac{n^2+2}{3} \right)^2 \sum_{l, \alpha} (e_l^{\alpha x})^2 \frac{1}{M_l}. \quad (36)$$

#### Calculation

Using the expression for the Green's function of a perfect lattice, Eq. (6), and the well-known formal relation

$$\lim_{\epsilon \rightarrow 0} (S - i\epsilon)^{-1} = \mathcal{P}1/S - i\pi\delta(S), \quad (37)$$

where  $\mathcal{P}$  denotes a principal value, the imaginary and real components of the perfect-crystal Green's function can be written

$$\lim_{\epsilon \rightarrow 0} \text{Im} g_{\alpha\beta}(l-l'; \omega^2 - i\epsilon) = \frac{\pi}{MN2\omega} \sum_{kj} E_{\alpha}(\mathbf{k}, j) E_{\beta}(\mathbf{k}, j) \cos(\mathbf{k} \cdot \mathbf{U}) \delta(\omega - \omega_j(\mathbf{k})) \quad (38)$$

$$\lim_{\epsilon \rightarrow 0} \text{Re} g_{\alpha\beta}(l-l'; \omega^2 - i\epsilon) = -\mathcal{P} \int_0^{\infty} \lim_{\epsilon \rightarrow 0} \text{Im} \frac{g_{\alpha\beta}(l-l'; \omega^2 - i\epsilon)}{\omega^2 - \omega'^2} d\omega'. \quad (39)$$

These expressions were evaluated using the following procedure. First, the eigenvalues and eigenvectors of the perfect crystal were found. Then Eq. (38) was used to find the imaginary part of the Green's function. The summation in this equation is over all values of  $\mathbf{k}$  in the first Brillouin zone (BZ). Actually, only 1/48 of the first BZ needs explicit consideration if one remem-

bers that the eigenvectors are changed in a trivial manner by a symmetry operation of the point group. It was decided that an examination of 1925 sample points in 1/48 of the BZ gave a reasonable compromise between numerical accuracy and computer time. The real part of the Green's function was found from the imaginary part using the dispersion integral, Eq. (39). The inversion of the  $4 \times 4$  matrix  $\mathbf{R}(1 - \mathbf{g}\delta)\mathbf{R}^{-1}$  in Eq. (33) was performed numerically.

The determination of suitable effective-charge parameters presents no difficulty for a charged defect. For the case of a deformable defect the effective charge could be found using Eq. (20), but we prefer to use a simple shell model.<sup>11</sup> In this model a point mass with charge  $f$  represents the nucleus and tightly bound electrons. This core is connected to a spherical shell with charge  $-f$  by a spring with force constant  $\gamma_c$ . Adjacent shells are connected by springs with force constant  $\gamma$ . In order to determine the effective charge of the symmetry coordinates of our defect molecule, we first find the effective charge  $e_l^{x\beta}$  corresponding to a displacement of each of the 13 atoms in the defect space. Since a displacement of a core will distort only its nearest neighbors in our approximation, we will have 78 simultaneous equations to solve for static equilibrium. However, the problem is greatly simplified by symmetry considerations and by the fact that  $\gamma_c$  is much greater than  $\gamma$ . Once the  $e_l^{x\beta}$ 's have been determined, it is an easy matter to use the symmetry coordinate transformation  $\mathbf{R}$  to find the effective charge of the symmetry coordinates  $e_m^x$ . If  $f'$  and  $\gamma_c'$  are, respectively, the core charge and core-shell spring constant of the defect atom, it can be shown that

$$e_1^x = 4\gamma' \left[ \frac{f'}{\gamma_c'} - \frac{f}{\gamma_c} \right]. \quad (40)$$

The effective charge of symmetry coordinate 1 is, of course, the effective charge of the defect atom. If we wish to find the effective charge of an atom which is farther from the defect atom than the defect's nearest neighbors, we would have the same problem to solve with the expectation that the center atom would be a host atom. In this case, of course,  $f'$  equals  $f$  and  $\gamma_c'$  equals  $\gamma_c$ . From Eq. (40) we have the important result that all atoms outside the space of the defect have zero effective charge. The effective charge of the three remaining symmetry coordinates are

$$\begin{aligned} e_2^x &= -\frac{1}{4}\sqrt{2}e_1^x, \\ e_3^x &= 0, \\ e_4^x &= +\frac{1}{4}\sqrt{2}e_1^x. \end{aligned} \quad (41)$$

Equation (33) will be put in a form more convenient for a calculation of the absorption coefficient of an arbitrary system. The actual Green's functions calcu-

<sup>10</sup> E. Wigner, Nachr. Akad. Wiss. Göttingen, Math.-physik. Kl. IIa. Math. physik. chem. Abt. **1930**, 133 (1930) [English transl.: R. S. Knox and A. Gold, in *Symmetry in the Solid State* (W. A. Benjamin, Inc., New York, 1964)].

<sup>11</sup> S. Doniach and R. Huggins, Phil. Mag. **12**, 393 (1965).

lated have the dimensionless form

$$g' = m\omega_L^2 g. \quad (42)$$

It is also convenient to express  $D$ , the density of defects, in the form of a percentage defect concentration  $P$ . That is,

$$P = \frac{1}{4} a^3 D \times 10^2, \quad (43)$$

where  $a$  is the lattice constant. Finally, the effective-charge parameters will be rewritten

$$e_i^x = \gamma \left[ \frac{f'}{\gamma_c'} - \frac{f}{\gamma_c} \right] E_i, \quad (44)$$

where

$$\begin{aligned} E_1 &= 4[1 - \Delta\gamma/\gamma], \\ E_2 &= -\sqrt{2}[1 - \Delta\gamma/\gamma], \\ E_3 &= 0, \\ E_4 &= \sqrt{2}[1 - \Delta\gamma/\gamma]. \end{aligned} \quad (45)$$

Using these new definitions, Eq. (33) takes the form

$$K(\omega) = T \frac{\omega}{\omega_L} \sum_{m, m'} E_m E_{m'} \lim_{\epsilon \rightarrow 0} \text{Im} \times \{ [\mathbf{R}^{-1}(\mathbf{1} - \mathbf{g}'\delta/M\omega_L^2)\mathbf{R}]^{-1} \mathbf{R}^{-1} \mathbf{g}' \mathbf{R} \}_{mm'}, \quad (46)$$

where

$$T = \frac{16\pi P e^2 \gamma^2}{10^2 a^3 c M \omega_L n} \left( \frac{n^2 + 2}{3} \right)^2 \left[ \frac{f'/e}{\gamma_c'} - \frac{f/e}{\gamma_c} \right]^2. \quad (47)$$

Most of the calculations will be for the case  $T=1$ . For a specific host-defect system the calculated curves can be scaled by the appropriate  $T$ .

### Results

For a lattice composed of deformable atoms, the dipole moment of a mode depends on the nuclear displacements of all 13 atoms in the space of the defect. This makes it difficult to interpret the absorption curves in terms of atomic motion. In an effort to mitigate this difficulty, we will first consider the model of a charged defect in a host of uncharged rigid atoms. In

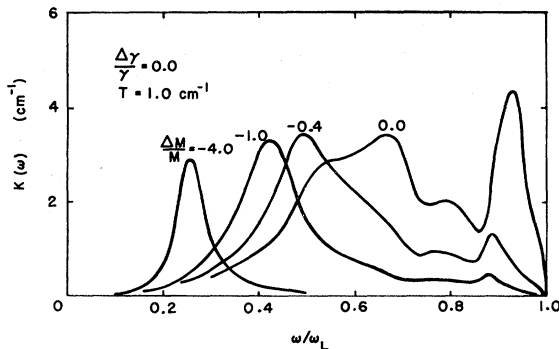


FIG. 3. Absorption coefficient  $K(\omega)$  for a charged defect  $\Delta\gamma/\gamma=0$ .

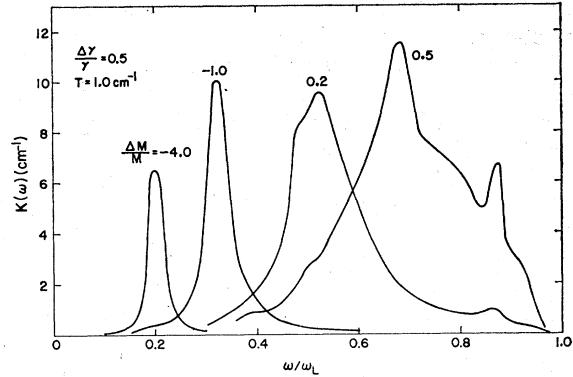


FIG. 4. Absorption coefficient  $K(\omega)$  for a charged defect  $\Delta\gamma/\gamma=0.5$ .

our calculation we can easily simulate this model by setting

$$\begin{aligned} E_1 &= 1, \\ E_2 &= E_3 = E_4 = 0. \end{aligned} \quad (48)$$

The absorption coefficient in this case will depend on the motion of only the defect atom and on the density of states.

For  $\Delta\gamma/\gamma = \Delta M/M = 0$  the lattice motion is, of course, that of the perfect crystal and the defect displacements are the same for every mode. The absorption coefficient is, therefore, proportional to the density of states. Figures 3-5 show the calculated absorption coefficient for a charged defect using this and other choices of defect parameters. The parameters have been chosen in these figures so that no localized mode exists. However, the resonance in the vicinity of 0.9 is closely related to the localized mode. Notice that this resonance slowly shifts to higher frequency and quickly increases in amplitude as the mass of the defect is decreased. Apparently there is a smooth transition from resonance to localized mode at  $\omega = \omega_L$ . Figure 2 shows the continuity of the movement of this peak during its transition from resonance to localized mode. In the harmonic approximation the localized mode-absorption coefficient is a  $\delta$  function of frequency. It would be surprising if the shape of the resonance did not asymptotically approach a  $\delta$  function as  $\omega/\omega_L$  approached 1.

There is another important peak that moves continuously from  $\omega/\omega_L = 0$  to  $\omega/\omega_L = 0.55$  as the defect mass is decreased. We will call this resonance  $A$ . At the frequency  $\omega/\omega_L \approx 0.55$ , resonance  $A$  disappears and another resonance,  $B$ , emerges at a slightly higher frequency,  $\omega/\omega_L = 0.65$ . Continuing to decrease the defect mass shifts resonance  $B$  to  $\omega/\omega_L = 0.7$ . There appears to be a weak stationary resonance  $C$  at  $\omega/\omega_L = 0.8$ . For completeness, we will call the high-frequency resonance  $D$  mentioned earlier. Figure 6 shows the shift of these resonances with changing defect-force constants.

Roughly, resonance  $D$  must correspond to modes in which the impurity vibrates against its neighbors, and resonance  $A$  must involve an in-phase motion. This

may be made plausible by examining the nature of the perfect-crystal modes in the respective frequency ranges of the resonances. For very heavy defect masses and weak defect spring constants, resonance  $A$  occurs at those modes with nearly the same frequency as an Einstein oscillator composed of the defect mass connected to stationary nearest-neighbor atoms.

If we assume that the lattice is composed of deformable atoms, modes for which there is a large displacement of the defect relative to its neighbors will have a nonzero effective charge even if the defect atom does not move. The modes with small wavelengths will have a large effective charge since the relative displacement of the defect will be great. These small-wavelength modes come at relatively high frequencies. A comparison of Figs. 3 and 7 shows this to be true. All trends discussed for the charged defect are seen in these curves and the previous discussion is applicable. In particular, the curves in Fig. 2 hold for both charged defects and deformable defects. The essential difference in the absorption-coefficient curves is that the frequency-dependent effective charge tends to push down the low-frequency absorption and enhance the high-frequency absorption for the deformable defect.

Jones and Woodfine have measured the infrared absorption of pure and impure solid argon.<sup>12</sup> They found that pure solid argon has no frequency-dependent absorption. This indicates that multiphonon processes are unimportant, since one-phonon absorption is forbidden in a monatomic fcc lattice. Absorption did occur when krypton and xenon were added in concentrations of about 1%. The model we have chosen for this calculation should describe the solid rare gases fairly well. For a comparison with experiment we must decide what values should be assigned to the parameters of the model. From Eq. (46) it is clear that the only parameters which will effect the shape of the absorption curve are  $\Delta\gamma/\gamma$ ,  $\Delta M/M$ , and  $\omega_L$ . The myriad of other parameters,  $P$ ,  $\gamma$ ,  $a$ ,  $n$ ,  $f'$ ,  $\gamma_c'$ ,  $f$ ,  $\gamma_c$ , merely define a constant  $T$  that determines the height of the curve. Estimating these latter parameters from other experi-

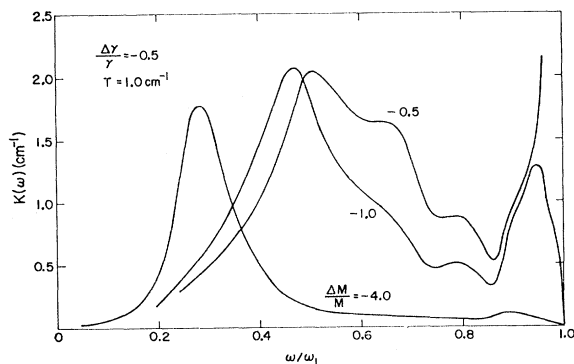


FIG. 5. Absorption coefficient  $K(\omega)$  for a charged defect,  $\Delta\gamma/\gamma = -0.5$ .

<sup>12</sup> G. O. Jones and M. Woodfine, Proc. Phys. Soc. (London) **86**, 101 (1965).

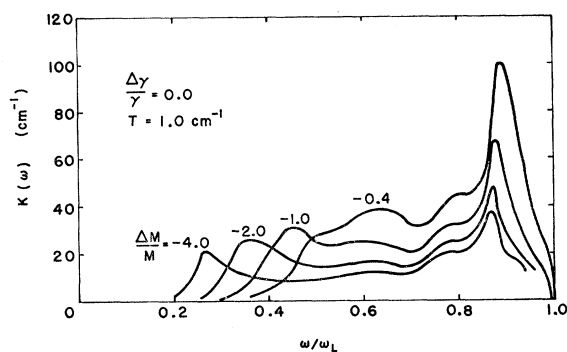


FIG. 6. Absorption coefficient for a deformable defect  $\Delta\gamma/\gamma = 0$ .

ments on solid rare gases is a rather arbitrary business since the shell model is such a crude description of a deformable atom. However, a very rough estimate of  $T$  may be made as follows. If we assume that an exciton can be described in our model as the motion of an otherwise noninteracting shell oscillating about its core, then the exciton frequency is

$$\omega_E^2 = \gamma_c / nm_e, \quad (49)$$

where  $n$  is the number of electrons in the shell. The corresponding effective charge is

$$f' = ne. \quad (50)$$

We have already indicated that in our model

$$\omega_L^2 = 8\gamma/M, \quad (51)$$

so

$$\frac{f/e}{\gamma_c/\gamma} = \frac{M}{8m_e} \left( \frac{\omega_L}{\omega_E} \right)^2. \quad (52)$$

Using  $8.5 \times 10^{-3}$  eV for  $\hbar\omega_L$ , 12.2 eV for  $(\hbar\omega_E)_{\text{Ar}}$ ,<sup>13</sup> and 9.2 eV for  $(\hbar\omega_E)_{\text{Ar:Xe}}$ ,<sup>13</sup> we find for 0.5% Xe in Ar,

$$T \approx 2 \times 10^{-4} \text{ cm}^{-1}. \quad (53)$$

The value of  $T$  used to fit the experimental curve was  $6 \times 10^{-4} \text{ cm}^{-1}$ .

Certainly, we may assume that the defect and host atomic masses are known. In fact, for the cases of interest,

$$\begin{aligned} (\Delta M/M)_{\text{Ar:Kr}} &= -1.10 \pm 0.05, \\ (\Delta M/M)_{\text{Ar:Xe}} &= -2.30 \pm 0.10. \end{aligned} \quad (54)$$

The uncertainty is due to the various isotopes, assuming they occur in a natural abundance. The limiting frequency  $\omega_L$  should be fairly well defined by the empirical absorption curve, since in an harmonic approximation there will be no absorption at frequencies higher than  $\omega_L$ , except at possible well-defined localized modes. A crude estimate of  $\Delta\gamma/\gamma$  may be made by examining the combining relations for the parameters of a 6-12 potential.<sup>14</sup>

<sup>13</sup> G. Baldini, Phys. Rev. **137**, A508 (1965).

<sup>14</sup> J. O. Hirschfelder, C. F. Curtiss, and R. B. Bird, *Molecular Theory of Gases and Liquids* (John Wiley & Sons, Inc., New York, 1954).

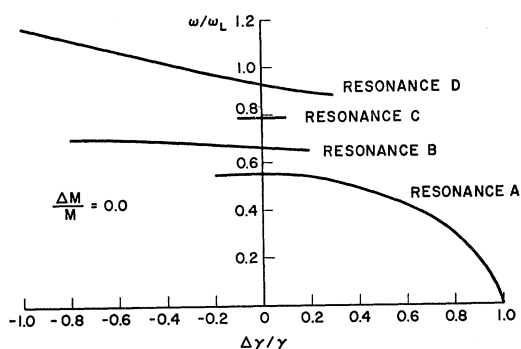
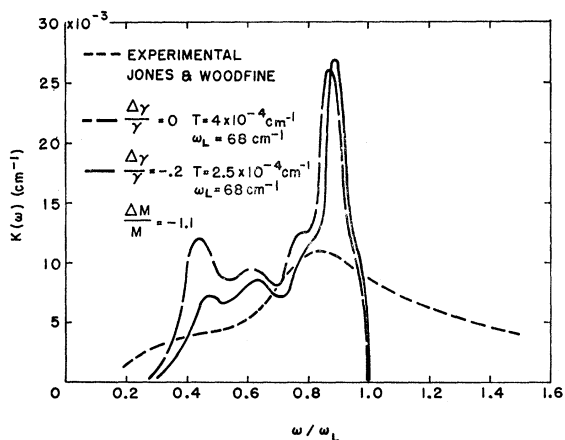
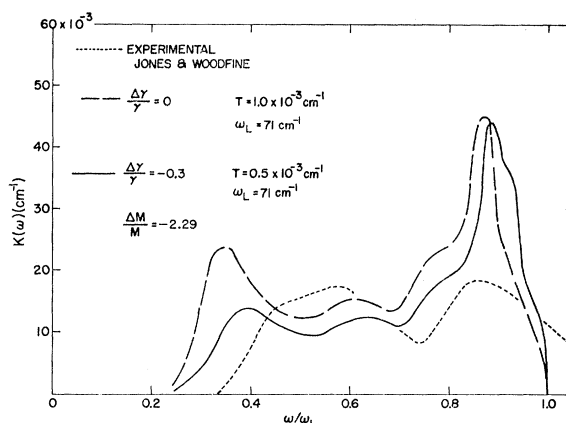
FIG. 7. Resonance frequencies for  $\Delta M/M = 0.0$ .

Figure 8 shows a comparison of the experimental curve of Jones and Woodfine for the Ar:Kr system and calculated curves using the indicated parameters. The experimental absorption extends far beyond  $\omega_L$ , indicating that anharmonic terms are very large. These measurements were made at relatively high temperatures, 80°K, which tends to enhance all anharmonic effects. Since our model is for a harmonic lattice, little can be said in comparing the curves. We would expect better agreement with an experimental curve taken at lower temperatures.

The experimental curve for the Ar:Xe system, Fig. 9, was obtained at 55°K. The absorption accordingly falls more rapidly for frequencies higher than  $\omega_L$ , but obviously anharmonic terms are still important. Crudely, one can approximate the effect of anharmonic terms on the calculated curves merely by imagining them to be damped in a uniform manner. Certainly, including a change in the nearest-neighbor force constant of the defect results in an improvement over the mass-defect calculation. It is worth emphasizing that the choice of the parameters in Fig. 9 were all physically realistic and that  $\Delta\gamma/\gamma$ ,  $\Delta M/M$ , and  $\omega_L$  were the only parameters effecting the shape of the curve.

Some of the more suspect assumptions which characterize our model are as follows:

FIG. 8. Comparison of the experimental and calculated absorption coefficient  $K(\omega)$  of Ar:Kr.FIG. 9. Comparison of the experimental and calculated absorption coefficient  $K(\omega)$  of Ar:Xe.

1. There is no static deformation of the lattice near the defect.
2. Terms in the electric moment quadratic in the displacements are negligible.
3. Only nearest neighbors interact.
4. The absorption coefficient due to  $N$  defects is  $N$  times the absorption coefficient due to one defect.
5. A rigid-atom model is used to evaluate the Green's functions and a shell model is used to evaluate the effective-charge parameters.
6. The interatomic potential is harmonic.
7. The effective-charge parameters can be estimated using the shell model.

Assumptions 1-4 are probably reasonable for the system considered. We found it convenient to assume rigid atoms in calculating the Green's functions of the perfect crystal and then to use the apparently contradictory shell model to estimate the effective charge parameters. Fortunately, there is a convenient way of checking the validity of this method. Hartmann has made a calculation of the absorption coefficient due to a mass defect in a fcc lattice using the shell model in obtaining the necessary Green's function as well as in obtaining the electric moment.<sup>8</sup> The good agreement between his calculation and a calculation based on our technique confirms our use of assumption 5. Presumably, assumption 6 can be made more valid by doing the experiment at low temperatures. This leaves assumption 7 as a probable cause for the disagreement with experiment.

#### ACKNOWLEDGMENTS

The author wishes to express his gratitude to Professor Albert Gold for his advice and encouragement during the course of this investigation. He wishes to thank Professor R. S. Knox for several helpful conversations. The author is grateful to Dr. B. Kagle, Professor A. A. Maradudin, Dr. W. Hartmann, and Professor R. J. Elliott for making available unpublished work pertinent to this problem, and to D. Healey for pointing out an error.